



# IJRASET

International Journal For Research in  
Applied Science and Engineering Technology



---

# INTERNATIONAL JOURNAL FOR RESEARCH

IN APPLIED SCIENCE & ENGINEERING TECHNOLOGY

---

**Volume: 11    Issue: VII    Month of publication: July 2023**

**DOI: <https://doi.org/10.22214/ijraset.2023.54766>**

**[www.ijraset.com](http://www.ijraset.com)**

**Call:  08813907089**

**E-mail ID: [ijraset@gmail.com](mailto:ijraset@gmail.com)**

# $\text{Ni}_2\text{P}_2\text{O}_7$ Thin Film Electrode for High Performance Supercapacitor Applications

S. Nivetha<sup>1</sup>, S. Prabakar<sup>2</sup>, R. T. Karunakaran<sup>3</sup>, M. Narendhera Ganth<sup>4</sup>, S. Dinesh<sup>5</sup>

<sup>1</sup>Department of Science and Humanities, Park College of engineering and Technology, Kaniyur- 641 659, Coimbatore, Tamilnadu, India

<sup>2, 3, 4</sup>Department of Physics, Government Arts College, Udumalpet – 642126, Tamilnadu, India

<sup>5</sup>Department of Physics, Selvam Arts & Science College, (Autonomous), Namakkal, Tamil Nadu, India

**Abstract:** The electrochemical performances of the supercapacitor essentially rely on electrode materials. The transition metal phosphates have been attracted as electrode material for energy storage in supercapacitor. A valley-like  $\text{Ni}_2\text{P}_2\text{O}_7$  thin film electrode is synthesized by economic and reproducible chemical bath deposition technique. The high specific capacitance of  $\text{Ni}_2\text{P}_2\text{O}_7$  is obtained as 548 F/g at current density 1 A/g. The electrode delivered enhanced energy density of 14.47 Wh k/g at a power density 0.16 kW k/g. The results indicate that  $\text{Ni}_2\text{P}_2\text{O}_7$  is an exemplary supercapacitor candidate and it would lead to productive research in future energy storage applications.

**Keywords:** Chemical bath deposition,  $\text{Ni}_2\text{P}_2\text{O}_7$ , Structural properties, thin film, Energy storage and conversion

## I. INTRODUCTION

In recent years, increasing necessity of high energy storage devices for high power application captures researcher's attention. Major requirements of high energy storage devices such as easiness to use, high stability and rapid release of electrical energy can be fulfilled by supercapacitor devices [1]. Several materials have been investigated by researchers for supercapacitor applications such as, transition metal oxides [2], hydroxides [3] phosphides [4] and sulfides [5-8]. Large quest exists always to explore new materials in order to achieve electrochemically stable material with high power and energy density and many are attracted towards transition metal phosphate for supercapacitor applications [9]. Transition metal phosphates are being studied extensively for last one decade and towards different applications as, viz., batteries [10-12], photocatalysis [13], sensors [14] and energy storage devices [15]. Recently, they are captivated for energy storage applications due to their high conductivity, earth abundance, large structural channels for electrolyte ions percolation and as they mainly afford stable structure due to phosphate-oxygen (P-O) covalent bond [16]. Among metal phosphates, nickel, cobalt and manganese materials are being highly probed for energy storage applications due to its inexpensive nature, excellent redox action, high specific capacitance, good stability and superior corrosion resistance. Inspired by the previous research outcome from these materials, binder-free  $\text{Ni}_2\text{P}_2\text{O}_7$  thin film is deposited on glass substrate as supercapacitive thin film electrode by following chemical route. The synthesized  $\text{Ni}_2\text{P}_2\text{O}_7$  thin film electrode is found to be a promising candidate with tuned morphology for supercapacitive applications.

## II. EXPERIMENTAL

The starting materials for the thin film deposition of  $\text{Ni}_2\text{P}_2\text{O}_7$  are of analytical grade from Sigma Aldrich. Glass substrates of dimension 1 cm × 3 cm are used for deposition of the thin film electrode material in the present work. Before deposition, the glass substrates are cleaned by ultrasonication in distilled water and acetone and subsequently dried in hot air oven. Then, 3M of  $\text{NiCl}_2 \cdot 6\text{H}_2\text{O}$ , 1M of  $\text{KH}_2\text{PO}_4$  and 0.5 M of  $\text{NH}_2\text{CONH}_2$  are dissolved in 50 ml of double distilled water and stirred upto homogeneous solution formation. The substrates are kept immersed in the prepared solution bath at 90 °C. The deposition and thin film formation of  $\text{Ni}_2\text{P}_2\text{O}_7$  are clearly visible after 1 hr. Hence, the thin film electrodes are drawn outside the bath rinsed with double distilled water. Further, they are dried and calcined at 500 °C for 30 minutes. The crystalline structure and phase formation of  $\text{Ni}_2\text{P}_2\text{O}_7$  thin film electrode are analyzed by X-ray diffraction (XRD) using Bruker D8 advance and the surface topologies are investigated by Atomic force microscopy (AFM) using SPM 600 - Agilent Technologies. The chemical state and binding energy of  $\text{Ni}_2\text{P}_2\text{O}_7$  thin film electrode is estimated by X-ray photoelectron spectroscopy (XPS) using ESCALAB 250 - Thermo Fisher Scientific. The supercapacitive properties of thin film electrode are studied using BioLogic SP-300 modular research grade Galvanostat / FRA electrochemical workstation in a three electrode system in 1 M KOH as an electrolyte.

### III. RESULTS AND DISCUSSION

#### A. Structural and Surface Topological Analysis

Fig. 1(a) shows the XRD pattern of  $\text{Ni}_2\text{P}_2\text{O}_7$  thin film electrode. All the diffraction peaks are perfectly indexed to monoclinic crystal system with space group  $\text{P}2_1/c$  (14) which matched well with JCPDS card (49-1082). Unit cell parameters are obtained from a least square refinement (LSR) of the XRD data. The LSR of the indexed pattern gives cell parameters:  $a = 4.553 \text{ \AA}$ ,  $b = 9.630 \text{ \AA}$ ,  $c = 4.897 \text{ \AA}$  and  $\beta = 95.675^\circ$ . The unit cell parameters of  $\text{Ni}_2\text{P}_2\text{O}_7$  are close to those of the JCPDS data ( $a = 4.465 \text{ \AA}$ ,  $b = 9.897 \text{ \AA}$ ,  $c = 5.207 \text{ \AA}$  and  $\beta = 97.509^\circ$ ). The lattice planes are indicated in XRD pattern corresponding to diffraction peaks. The peak marked with ‘\*’ is related to glass substrates. The sharp intense peaks imply a good crystallinity of thin film electrode without any other impurity peaks in the XRD pattern indicating phase purity [17-19]. The average crystallite size (D) is estimated using the Debye-Scherrer relation and obtained average crystallite size is 37.68 nm. The three dimensional (3D) AFM image depicts the valley like structure of the film surface and sharp hill with the agglomerated particles (Fig. 1(b)). It exhibits a highly dense state topography with good crystallinity and the root mean square roughness ( $R_{\text{rms}}$ ) of the film is found to be 80.56 nm [20].

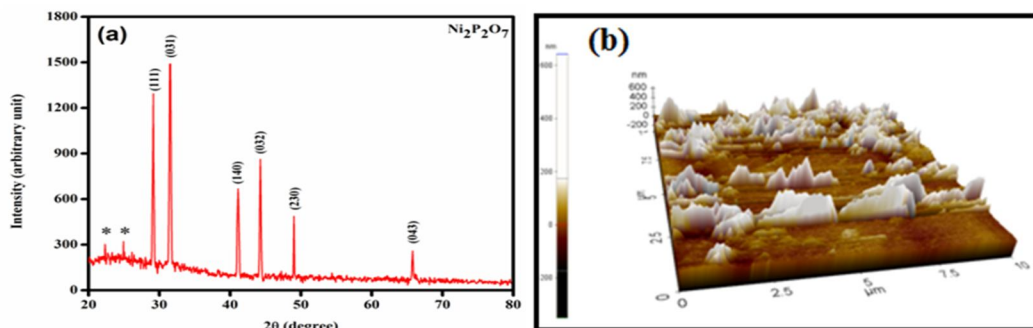


Fig. 1. (a) XRD pattern (b) AFM image of  $\text{Ni}_2\text{P}_2\text{O}_7$  thin film electrode

#### B. XPS

Fig. 2(a) shows XPS survey spectra of  $\text{Ni}_2\text{P}_2\text{O}_7$  thin film which indicates the presence of Ni, P and oxygen (O) species. The high resolution spectra of Ni 2p segment ( Fig. 2(b)) displays the two major peaks at 857.5 and 875.2 eV binding energies which correspond to the Ni  $2p_{3/2}$  and Ni  $2p_{1/2}$  along with two shakeup satellite peaks observed at 863.1 and 881.6 eV, respectively, which is the demonstration of  $\text{Ni}^{2+}$  in  $\text{Ni}_2\text{P}_2\text{O}_7$ . Fig. 2(c) shows XPS spectra of P 2p segment, only one major peak at the binding energy of 134.8 eV which is assigned to P-O bonding. Moreover, the strong and intense peak at 532.6 eV in the O 1s segment ( Fig. 2(d)), are assigned to metal oxygen bonding (Ni-O and P-O). All the above results indicate that the successful formation of  $\text{Ni}_2\text{P}_2\text{O}_7$  thin film with results in good agreement with earlier reports [21, 22].

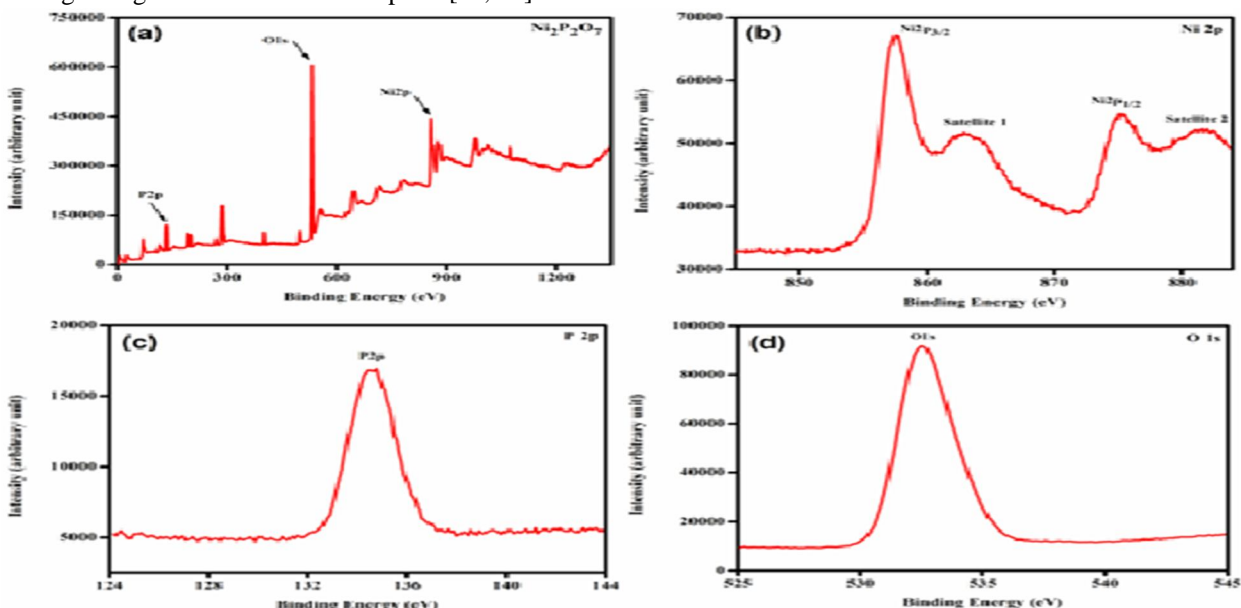


Fig. 2. (a) XPS survey spectra (b) Ni 2p spectra (c) P 2p spectra (d) O 1s spectra of the  $\text{Ni}_2\text{P}_2\text{O}_7$  thin film electrode.



### C. Super Capacitive Properties

Fig. 3(a) shows the cyclic voltammogram (CV) of  $\text{Ni}_2\text{P}_2\text{O}_7$  thin film electrode within the potential range of -0.4 to 0.2 Vs Hg/HgO at different scan rate 10-50 mV/s. A strong pair of redox peaks in CV profile confirms the combination of both pseudocapacitive and electrochemical double layer capacitive (EDLC) nature of the electrode [17, 23]. The specific capacitance of the electrode material is estimated using galvanostatic charge-discharge (GCD) profile in the potential range of 0.2 Vs Hg/HgO at various current densities shown in the Fig. 3(b). The GCD profile displays the specific capacitance values, as 548, 434, 385, 320, 283 and 183 F/g at 1, 2, 3, 4, 5 and 10 A/g, respectively, which are on higher side compared to those reported for  $\text{Ni}_2\text{P}_2\text{O}_7$  (Table 1). The increase in current density, specific capacitance of electrode decreases as decreasing discharging time and at low current density offers higher specific capacitance. The quasi-linear shape of GCD profile in all current densities depicts a slow potential decay in electrodes which is due to deep ion intercalation, evincing the faradaic reaction influence of the electrode material [24]. Electrochemical impedance spectroscopy (EIS) is carried out in the frequency range of 100 mHz to 1MHz with amplitude of 5mV and represented in the Nyquist plot shown in the Fig. 3(c), there is absence of semicircle in the high-frequency region and linear line observed at lower frequency region which indicates very small transfer resistance also called as Warburg diffusion resistance ( $W_R$ ) and fast electrochemical reactions. Lower the internal resistance greater will be the electrical conductivity [25, 26]. Ragone plot is shown Fig. 3(d), the energy density of electrode decreases from 14.47 to 0.491 Wh k/g and power density increases from 0.16 to 1.96 kW k/g with increasing GCD current density from 1 to 10 A/g [27]. It is obvious from this study that  $\text{Ni}_2\text{P}_2\text{O}_7$  thin film electrode offers excellent electrochemical performance.

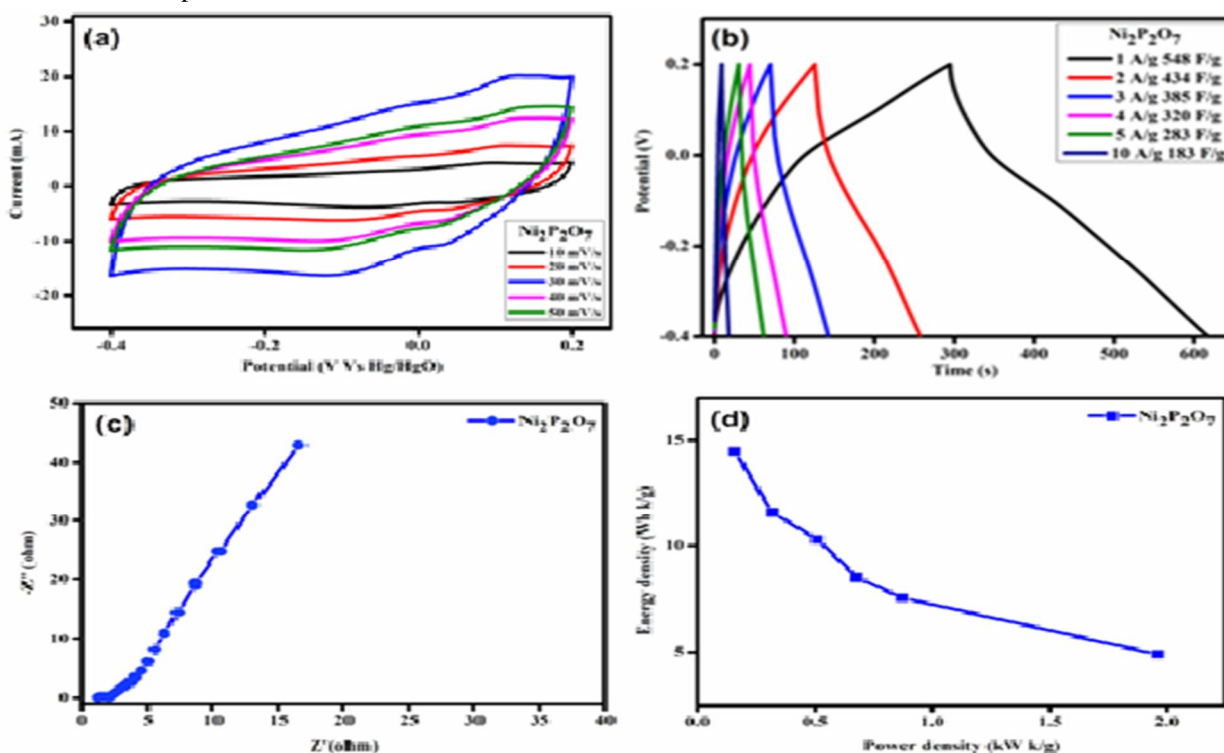


Fig. 3. (a) CV profiles of  $\text{Ni}_2\text{P}_2\text{O}_7$  thin film electrode at different scan rates (b) GCD profiles shows specific capacitance of  $\text{Ni}_2\text{P}_2\text{O}_7$  thin film electrode as a function of current densities (c) Nyquist plot at open circuit potential (d) Ragone plot..

Electrode	Electrolyte	Current density (A/g)	Specific capacitance (F/g)	Ref.
$\text{Ni}_3(\text{PO}_4)_2\text{-Ag}_3\text{PO}_4/\text{NF}$	1M KOH	0.5	146	[16]
$\text{Ni}_3(\text{PO}_4)_2/\text{NF}$	1M KOH	0.4	355	[18]
$\text{Ni}_2\text{P}_2\text{O}_7/\text{NF}$	1M KOH	1	224	[19]
$\text{Ni}_2\text{P}_2\text{O}_7/\text{TF}$	1M KOH	1	548	Present work

Table.1. Comparison of specific capacitance of the as-prepared  $\text{Ni}_2\text{P}_2\text{O}_7$  in the present work with other reported nickel phosphates Specification: NF – Nickel Foam, TF – Thin Film

#### IV. CONCLUSION

$\text{Ni}_2\text{P}_2\text{O}_7$  thin films with valley like topology are successfully deposited onto glass substrates and incorporated as a binder-free active electrode in electrochemical tests. XRD analysis establishes that the prepared film is monoclinic with high crystalline purity. The prepared electrode delivers utmost specific capacitance of 548 F/g at 1 A/g current density with energy density and power density values 14.47 Wh k/g and 0.16 kW k/g, respectively. The experimental results pertaining to the thin film synthesized by simple and standardized CBD method in the present work announces the film as a promising electrode material which would be beneficial for future energy requirements in supercapacitor domain.

#### REFERENCES

- [1] Y. Shao, M. El-Kady, J. Sun, Y. Li, Q. Zhang, M. Zhu, H. Wang, B. Dunn, R. Kaner, *Chem.Rev.* 118 (2018) 9233–9280.
- [2] B. M. Chong, N. H. N. Azman, *Appl. Sci.* 9 (2019) 1040-1051.
- [3] U. Patil, K. Gurav, J. Kim, C. Lokhande, S. Jun, *Bull. Mater. Sci.* 37 (2014) 27–33.
- [4] S. Liu, K. Sankar, A. Kundu, M. Ma, J. Kwon, S. Jun, *Appl. Mater. Interfaces* 9 (2017) 21829–21832.
- [5] X. Yu, L. Yu, H. Wu, X. Lou, *Angew. Chem. Int. Ed.* 54 (2015) 5331–5335.
- [6] Prabahar S, Dhanam M, *Journal of crystal growth* 285 (2005) 41-48.
- [7] Anis F.A, Nivetha S, Prabahar S, Srikanth S, Karunakaran R.T, Karunanithi U, Narendhera ganth M, *IJRASET.* 9 (2021) 242-245.
- [8] Anis F.A, Nivetha S, Prabahar S, Srikanth S, Karunakaran R.T, Karunanithi U, Narendhera ganth M, *IJRASET.* 9 (2021) 646-650.
- [9] C. Wei, S. Yang, W. Liu, X. Hou, Y. Sun, W. Xiong, C. Cheng, D. Zhang, *Appl. Surf. Sci.* 465 (2019) 763–771.
- [10] C. L. Li, B. Zhang, Z.W. Fu, *J. Electrochem. Soc.* 153 (2006) 160-165.
- [11] Nivetha S, Prabahar S, Karunakaran R.T, Narendhera ganth M, Dinesh S, *Inorganic Chem. Commun.* 146 (2022) 110193.
- [12] Nivetha S, Prabahar S, Karunakaran R.T, Narendhera ganth M, Dinesh S, *Chemistry Select* 8 (2023) 00535.
- [13] S. Marje, P. Katkar, S. Kale, A. Lokhande, C. Lokhande, U. Patil, *J. Alloys Compd.* 779(2019) 49–58.
- [14] S. Darzi, M. Esfidvajani, *J. Porous Mater.* 24 (2017) 85–95.
- [15] B. Li, P. Gu, Y. Feng, G. Zhang, K. Huang, H. Xue, H. Pang, *Adv. Funct. Mater.* 27 (2017) 1605784–1605795.
- [16] X. Li, A. Elshahawy, C. Guan, J. Wang, *Small* 13 (2017) 1701530–1701554.
- [17] X. Peng, H. Chai, Y. Cao, Y. Wang, H. Dong, D. Jia, W. Zhou, *Mater. Today Energy* 7 (2018) 129-135.
- [18] N. Padmanathan, H. Shao, K. M. Razeeb, *Appl. Mater. Interfaces* 10 (2018) 8599-8610.
- [19] Nivetha S, Prabahar S, Karunakaran R.T, Narendhera ganth M, Dinesh S, *Ionics* 29 (2023) 1209-1219.
- [20] M.F. Al-Kuhaili, S.H.A. Ahmad, S.M.A. Durrani, M. M.Faiz, A.Ul-Hamid, *Mater. Sci. Semicond. Process.* 39 (2015) 84–89.
- [21] S. Marje, P. Katkar, S. Pujari, S. Khalate, P. Deshmukh, U. Patil, *Mater. Sci. Eng. B* 261 (2020) 114641-114651.
- [22] F. Omar, A. Numan, S. Bashir, N. Duraisamy, R. Vikneswaran, Y.L. Loo, K. Ramesh, S. Ramesh, *Electrochim. Acta* 273 (2018) 216-228.
- [23] C. Cheng, Y. Cheng, G. Lai, *Mater. Lett.* 317 (2022) 132102.
- [24] K. Subramani, M. Sathish, *Sci. Rep.* 9 (2019) 1104-1127.
- [25] J. Wen, S. Li, T. Chen, B. Li, L. Xiong, Y. Guo, G. Fang, *Electrochim. Acta* 258 (2017) 266-273.
- [26] Narendhera ganth M, Prabahar S, Karunakaran R.T, Nivetha S, Dinesh S, (2023) Doi: <http://doi.org/10.1007/s11581-023-05065-0>.
- [27] S. Marje, P. Katkar, S. Pujari, S. Khalate, A. Lokhande, U. Patil, *Synth. Met.* 259 (2020) 116224-116235.



10.22214/IJRASET



45.98



IMPACT FACTOR:  
7.129



IMPACT FACTOR:  
7.429



# INTERNATIONAL JOURNAL FOR RESEARCH

IN APPLIED SCIENCE & ENGINEERING TECHNOLOGY

Call : 08813907089  (24\*7 Support on Whatsapp)